IOPscience iopscience.iop.org

Home Search Collections Journals About Contact us My IOPscience

Structural and dynamical properties of α-CuI: a molecular dynamics study

This article has been downloaded from IOPscience. Please scroll down to see the full text article.

1997 J. Phys.: Condens. Matter 9 1477

(http://iopscience.iop.org/0953-8984/9/7/012)

View the table of contents for this issue, or go to the journal homepage for more

Download details:
IP Address: 171.66.16.207
The article was downloaded on 14/05/2010 at 08:07

Please note that terms and conditions apply.

J. Phys.: Condens. Matter **9** (1997) 1477–1492. Printed in the UK PII: S0953-8984(97)76912-1

Structural and dynamical properties of α-CuI: a molecular dynamics study

K Ihata† and H Okazaki‡

† Graduate School of Science and Technology, Niigata University, Niigata 950-21, Japan
‡ Department of Physics, Niigata University, Niigata 950-21, Japan

Received 5 August 1996, in final form 28 October 1996

Abstract. A constant temperature–constant volume molecular dynamics simulation has been applied to superionic CuI (α-CuI) with the use of a pairwise interionic potential. Excellent agreement between the calculated value D_{cal} and experimental value D_{exp} of the cation diffusion coefficient is obtained. About 35% of cations are resident in octahedra formed by cage ions (I ions) but a small cation occupation at octahedral sites was found. The remaining cations are distributed among tetrahedra including T_+ and T_- sites with different weights, where T_+ and T_- denote tetrahedral sites which are occupied by ions and vacant in the zincblende structure, respectively. The jump frequency Γ and the correlation factor f of mobile ions are evaluated with the use of the polyhedron analysis method. Quantities D_{cal}, Γ and f evaluated by the simulation reproduce well the relation $D_{cal} = \Gamma r^2 f/6$ under the assumption of constant r.

1. Introduction

In the earlier stages of molecular dynamics (MD) simulation being applied to superionic conductors, Vashishta and Rahman [1] performed the simulation of CuI, which has three polymorphisms in the solid state: the γ-phase below 658 K, the β-phase between 658 and 680 K and the α-phase between 680 K and the melting point 873 K. In the γ- and α-phases, anions form FCC structures. In the former phase, cations occupy half of the tetrahedral sites (hereafter referred to as T_+ sites) so as to form a zincblende structure and in the latter cations are distributed over tetrahedral sites, not only T_+ but also T_- sites which are vacant sites in the γ-phase, and over octahedral sites. β-CuI has a hexagonal structure described in [8, 19].

They succeeded in reproducing the structure of the γ- and α-phases and in obtaining semiquantitative agreement between the calculated and experimental values of the cation diffusion coefficient. They also derived roughly the cation distribution in the α-phase along various directions of structure and pointed out the probable path of cations in diffusion.

Recently, Trullàs *et al* [2] have performed the MD simulation of α-CuI with the use of the interionic potential used by Vashishta and Rahman. They investigated the effect of the effective charge on its crystal structure and on the superionic characteristic. However, they did not obtain good agreement between the calculated and experimental diffusion coefficient [3, 4].

A fairly good agreement between calculated and experimental values of the cation diffusion coefficient was obtained by Johansson *et al* [5, 6]. They also used the same form of the interionic potential as used by Vashishta and Rahman, but values of parameters appearing in the potential were different from those of Vashishta and Rahman. Their calculations were

0953-8984/97/071477+16$19.50 © 1997 IOP Publishing Ltd

carried out for three polymorphisms of CuI and contour maps of the cation distribution and the characteristic behaviour of the ion in each phase were derived. Although some MD calculations for CuI were reported, we consider that it is worth examining again the MD calculation for the present material, since the quantitative agreement between calculated and experimental values of the cation diffusion coefficients is not yet close enough and quantitative analysis of the diffusion mechanism has not been given.

In the present work, our interest is concentrated on α-CuI, since it shows highly ionic conduction and its distribution of Cu ions is very disordered. The purposes of the present study are: (1) to improve the quantitative agreement between the calculated and experimental values of the cation diffusion coefficient; (2) to analyse the crystal structure in detail, especially the distribution of cations within the tetrahedron and octahedron formed by the anion FCC lattice; and (3) to elucidate the microscopic behaviour of mobile ions in diffusion.

As one way to realize the above aims, we adopt the polyhedron analysis method, which gives a powerful approach for investigating the diffusion phenomenon in partially disordered systems such as superionic conductors. In section 4, we describe the method in detail and show the usefulness of the method.

2. Calculation

The effective interionic potential, V_{ij}, used in the calculation is of the form proposed by Vashishta and Rahman in the simulation for the same material [1],

$$V_{ij} = \frac{q_i q_j}{r} + \frac{H_{ij}}{r^{n_{ij}}} - \frac{P_{ij}}{r^4} - \frac{W_{ij}}{r^6} \tag{1}$$

with

$$H_{ij} = A(\sigma_i + \sigma_j)^{n_{ij}} \qquad \text{and} \qquad P_{ij} = \tfrac{1}{2}(\alpha_i q_j^2 + \alpha_j q_i^2)$$

where σ_i, q_i and α_i are the ionic radius, the effective charge and the electronic polarizability of the ith ion, respectively. The effective charge q_i is expressed as $q_i = z_i e$, where z_i is the effective valence and e the elementary charge. After some trial calculations, parameters appearing in equation (1) are determined as $z_{Cu} = 0.70$ $(= -z_1)$, which is used instead of 0.60 assumed by Vashishta and Rahman, with the values of other parameters taken to be the same as those used by Vashishta and Rahman. In table 1, values of parameters are summarized with those used by Johansson *et al* [5, 6].

The calculations are carried out using the standard constant volume (NVE) algorithm with a constant temperature method. In order to maintain the system (MD cell) at a settled temperature during the calculation, we solved the following simultaneous differential equations in each time step [7],

$$\frac{\mathrm{d}\boldsymbol{r}_i}{\mathrm{d}t} = \frac{\boldsymbol{p}_i}{m_i} \tag{2}$$

$$\frac{\mathrm{d}\boldsymbol{p}_i}{\mathrm{d}t} = -\sum_{j\neq i} \frac{\partial V_{ij}}{\partial \boldsymbol{r}_{ij}} - \zeta \boldsymbol{p}_i \tag{3}$$

$$\frac{\mathrm{d}\zeta}{\mathrm{d}t} = \frac{1}{Q}\left(\sum_{i=1}^{N} \frac{\boldsymbol{p}_i^2}{m_i} - 3Nk_BT\right) \tag{4}$$

where m_i, $\boldsymbol{r}_i$ and $\boldsymbol{p}_i$ are the mass, position vector and momentum of the ith particle, respectively. ζ is a 'friction' constant to prevent the temperature of the system deviating from the settled temperature T and Q is a parameter relating to the heat bath, having the dimension of mass. The value of Q used in the present calculation is also given in table 1.

Table 1. Values of the parameters appearing in the effective interionic potential (those in parentheses are used by Johansson *et al* [5, 6]).

q_{Cu}	0.70 (0.81) e	n_{CuCu}	7 (7.3)
q_I	-0.70 (−0.81) e	n_{CuI}	7 (7.3)
		n_{II}	7 (7.3)
σ_{Cu}	0.53 (0.450) Å	H_{CuCu}	0.011 96[a] (0.006 060)
σ_I	2.10 (2.188) Å	H_{CuI}	12.982[a] (51.657)
		H_{II}	399.578[a] (2078.182)
α_{Cu}	0.00 (0.00) Å^3	W_{CuCu}	0.00 (2.25)
α_I	6.52 (7.00) Å^3	W_{CuI}	0.00 (2.25)
		W_{II}	99.79 (2.25) (eV Å^6)
Q	6.24 (kJ mol^{-1} ps^2)		

[a] Given in units of e^2 Å^{-1} (=14.39 eV).

The MD cell is formed in a cube of side L with $4 \times 4 \times 4$ FCC unit cells, where 512 particles with 256 I and 256 Cu ions are included. The value of L is set at 24.60 Å at 760 K and a small correction according to the thermal dilatation ($7.0 \times 10^{-5}\,^{\circ}\mathrm{C}^{-1}$) [8] is made for other temperatures. I ions are put on the FCC lattice points and Cu ions are initially put on T_+ sites so as to form the zincblende structure.

Simulations are carried out for three temperatures, 700, 760 and 840 K. At each temperature, calculations are performed for 20 000 time steps, where one time step is 5.0×10^{-15} s. The periodic boundary condition is applied and the Ewald sum method is also used for calculating the Coulomb interaction. The calculation for the initial 4000 time steps is considered for stabilizing the system and data after 4000 time steps are used for deriving physical quantities of interest.

3. Results

3.1. Mean square displacements

The mean square displacements (MSD) of anions and cations as functions of time for three temperatures are shown in figure 1, which shows that anions form a lattice stably while cations migrate far from the region of interionic distance (∼2.7 Å), resulting in the diffusion of cations. The diffusion coefficients, D, are evaluated from the inclination of the linear relation between the MSD and time (t_1 to t_2) by the relation

$$D = \langle [\boldsymbol{r}(t_2) - \boldsymbol{r}(t_1)]^2 \rangle / 6(t_2 - t_1) \tag{5}$$

where $\boldsymbol{r}(t)$ means the position vector of a cation at time t. Values of D evaluated by equation (5) are shown by full circles in figure 2, in which experimental values obtained by a tracer method [3, 4] and calculated values of Vashishta and Rahman are given by open circles and full squares, respectively. Calculated values of Johansson *et al* are also given in figure 2 by open squares. The agreement between the calculated and the experimental values is excellent.

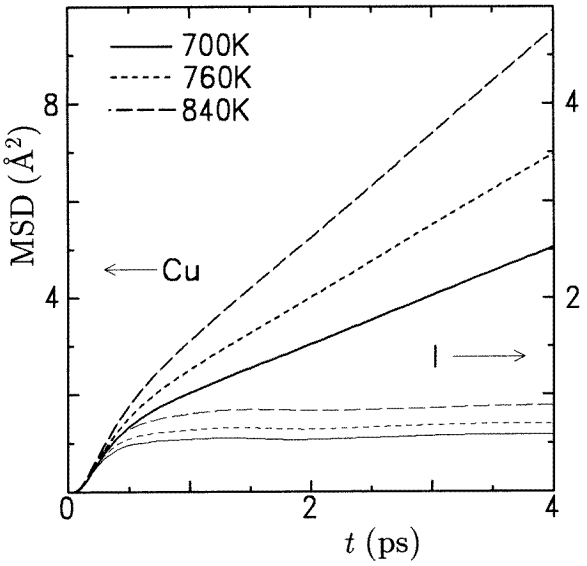

Figure 1. Mean square displacements of Cu ions and I ions at 700, 760 and 840 K. Bold and thin lines are for Cu and I ions, respectively.

3.2. Partial pair distribution functions

Three partial pair distribution functions, $g_{II}(r)$, $g_{ICu}(r)$ and $g_{CuCu}(r)$ are calculated and those at 760 K are shown in figure 3. The form of $g_{II}(r)$ corresponds to that of the FCC structure. The curve of $g_{ICu}(r)$ shows that Cu ions are strongly localized near the I ion in a small region (∼0.8 Å). Its first peak position (2.30 Å) is shorter than both $(\sigma_I + \sigma_{Cu}) = 2.63$ Å and the distance between a FCC lattice point and its neighbouring tetrahedral site (2.66 Å). It is seen from $g_{CuCu}(r)$ that the distribution of the Cu ion is quite liquid-like. The first peak position of $g_{CuCu}(r)$ is 4.1 Å, which is close to the distance between neighbouring T_+ sites (4.35 Å). Thus, it might be said that the structure of α-CuI fundamentally remains in the zincblende structure.

The coordination numbers, $n_{\alpha\beta}$, the average number of α ions around a β ion, are evaluated by the equation

$$n_{\alpha\beta} = 4\pi\rho_0 c_\alpha \int_0^{r_{min}} r^2 g_{\alpha\beta}(r)\,\mathrm{d}r$$

where ρ_0 is the number density of ions, c_α the ratio of the number of α ions to the total number of ions and r_{min} the first minimum position of the distribution function. In table 2,

Table 2. Value of the first minimum of $g_{\alpha\beta}(r)$ and coodination numbers $n_{\alpha\beta}$ (α, β = Cu, I).

		Temperature (K)		
	r_{min} (Å)	700	760	840
n_{II}	5.40 ± 0.10	12.03 ± 0.20	12.04 ± 0.20	12.04 ± 0.20
n_{CuI}	3.50 ± 0.10	3.55 ± 0.10	3.53 ± 0.11	3.51 ± 0.11
n_{CuCu}	5.45 ± 0.15	11.57 ± 0.64	11.28 ± 0.70	11.06 ± 0.77

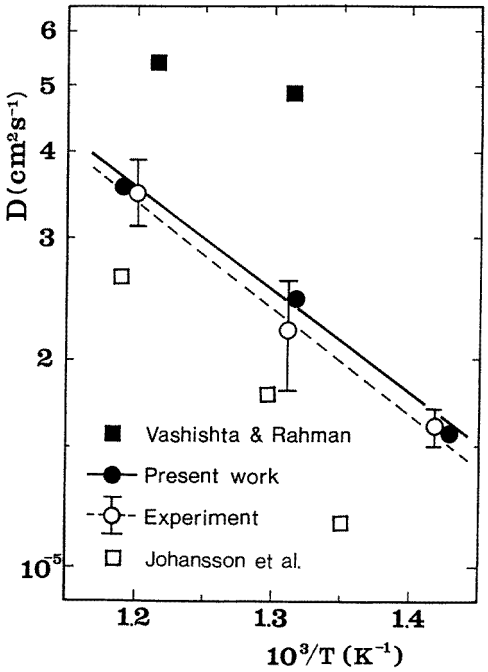

Figure 2. Arrhenius plots of diffusion coefficients evaluated from MSDs represented by full circles and those obtained by the tracer measurement by open circles. Full and open square marks are diffusion coefficients obtained by Vashishta and Rahman [1] and Johansson *et al* [5, 6], respectively.

values of $n_{\alpha\beta}$ and r_{min} are given, where a single value of r_{min} at 760 K is cited since the temperature dependence of r_{min} was negligible. The value of n_{II} remains at 12 for the three temperatures, which means that iodines form a stable FCC structure. The value of n_{ICu} is a little smaller than four and decreases with temperature, which shows that smaller numbers of Cu ions leave from the tetrahedral site towards the octahedral one. Values of n_{CuCu} also decrease slightly with temperature and the temperature dependence of n_{CuCu} and n_{ICu} means that the population of Cu ions at tetrahedral sites decreases with temperature.

In figure 4, the density distribution of Cu ions on the (110) plane at 760 K is shown by a bird's-eye view picture. From the figure it can be seen that Cu ions distribute not only on T_+ sites but also T_- sites. We also find that there are no peaks at octahedral sites. The figure suggests that cations stay for the majority of the time at tetrahedral sites with asymmetric and anharmonic thermal vibrations but sometimes penetrate forward octahedral sites overcoming the barrier formed by the anion triangle. This situation will be analysed in detail by the polyhedron analysis method later.

3.3. Velocity autocorrelation functions

The normalized velocity autocorrelation function (VAF), $Z_\alpha(t)$, of an α-ion species defined as

$$Z_\alpha(t) = \langle \boldsymbol{v}_\alpha(t) \cdot \boldsymbol{v}_\alpha(0) \rangle / \langle \boldsymbol{v}_\alpha^2(0) \rangle. \tag{6}$$

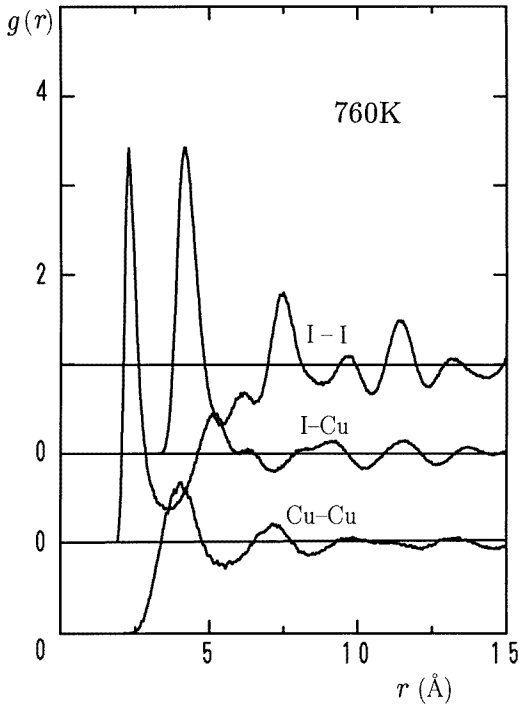

Figure 3. Partial pair distribution functions $g_{\alpha\beta}(r)$ (α, β = I, Cu) at 760 K.

is evaluated, where $v_\alpha(t)$ shows the velocity of an α-ion at time t and $\langle\ \rangle$ denotes the average taken for α-ions included in the MD cell. The vibrational density of state, $G_\alpha(\omega)$, is given by the Fourier transformation of $Z_\alpha(t)$

$$G_\alpha(\omega) = \int_0^\infty Z_\alpha(t) \cos \omega t \, \mathrm{d}t. \tag{7}$$

In figures 5(*a*) and 5(*b*), $Z_\alpha(t)$ and $G_\alpha(\omega)$ at 760 K are shown, respectively. The diffusion coefficient of the Cu ion may also be evaluated from equation (7) by the relation

$$D_{Cu} = \frac{k_B T}{m_{Cu}} G_{Cu}(\omega = 0). \tag{8}$$

Those derived from equation (8) are 1.77 (1.56), 2.74 (2.45) and 3.78 (3.55) in units of 10^{-5} cm^2 s^{-1} at 700, 760 and 840 K, respectively, where values in the parentheses are those obtained from the MSD. Diffusion coefficients evaluated from $G_{Cu}(\omega = 0)$ are a little larger than those from MSD, and we use the latter as the self-diffusion coefficients, since the latter are more reliable than the former because of the truncation in the integration of $Z(t)$.

4. Polyhedron analysis

4.1. Polyhedron analysis

The polyhedron analysis [9–11] is one useful method for analysing the microscopic behaviour of mobile ions (atoms) in highly disordered solids such as superionic conductors,

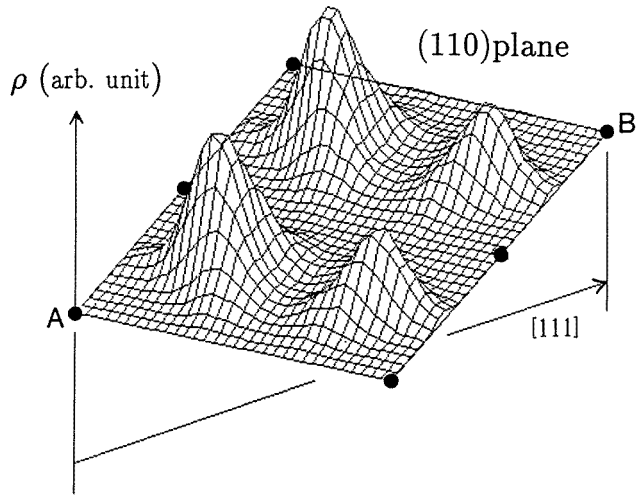

Figure 4. Bird's-eye view of the Cu ion density distribution in the (110) plane at 760 K. Small circles indicate the position of anions. The crystal direction [111] runs from point A to point B.

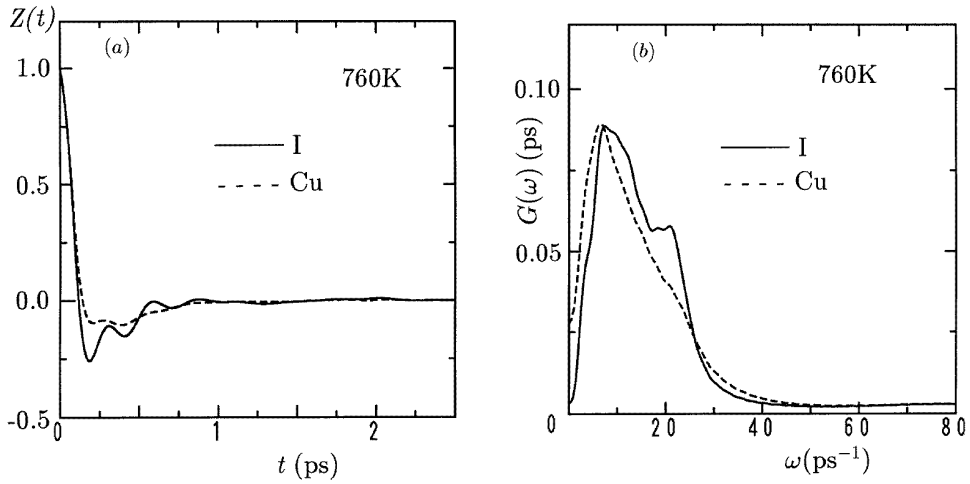

Figure 5. (*a*) Velocity autocorrelation functions $Z(t)$ and (*b*) frequency spectra $G(\omega)$ at 760 K. Full and broken lines are for anion and cation, respectively.

where immobile ions form a lattice while mobile ions do not have their own stable sites and go around in space constructed by the lattice ions. For the diffusion phenomenon in such materials the ordinary diffusion theory of solids is not applicable, since the theory is based on the idea that the diffusion results from a number of ion jumps between stable sites for ions, in which the jump frequency and the jump distance are clearly defined.

In this method, the space available for the ion migration is divided into a few kinds of polyhedron constructed by connecting neighbouring cage ions. When we regard a movement of a mobile ion from a polyhedron to another polyhedron as a 'jump' of the ion, we can

deal with the ion migration in superionic conductors by means of the ordinary diffusion theory of solids.

For the case of α-CuI, cage ions form a FCC structure and the space for mobile ions is decomposed into two kinds of polyhedron, tetrahedron and octahedron, as shown in figure 6. For the zincblende structure, the tetrahedra are divided into two kinds, $\oplus$ and $\ominus$ tetrahedra, which include T_+ and T_- sites, respectively. Each FCC unit cell includes eight tetrahedra and four octahedra. A tetrahedron is connected with an octahedron through a regular triangle and with other tetrahedra through an edge. An octahedron is linked with a neighbouring octahedron through an edge or through a point which is one of the FCC lattice points. Thus, three paths are probable for the ion migration: (1) from tetrahedron to octahedron through the common triangle and *vice versa*; (2) from tetrahedron to tetrahedron through their common edge; and (3) from octahedron to octahedron through their common edge. We found by analysing trajectories of mobile ions in detail that the path (1) is most probable. The migration through the common edge-sharing tetrahedra or octahedra (paths (2) and (3)) was observed infrequently. Thus, it is enough to consider only the ion migration between tetrahedron and octahedron.

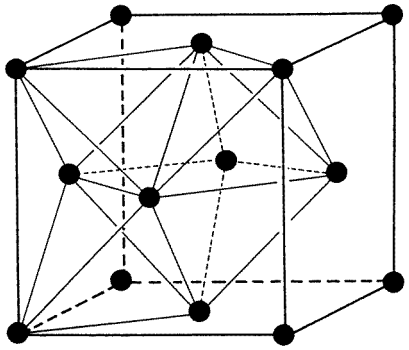

Figure 6. Lattice points in a FCC unit cell and two kinds of polyhedron (tetrahedra and octahedra) formed by connecting neighbouring lattice points.

4.2. Distribution of cations among polyhedra

As described in section 2, the calculation begins with the situation that Cu ions are initially put on T_+ sites. Hereafter, we describe the position of each Cu ion by a tetrahedron or octahedron including the respective ion instead of the position vector. After the calculation starts, some of the Cu ions soon move to octahedra from their respective initial tetrahedra, and an equilibrium distribution of Cu ions in tetrahedra and octahedra is realized after about 4000 time steps (20 ps). When the numbers of tetrahedra and octahedra including Cu ions are denoted by N_T and N_O, respectively, the time variation of N_T and N_O between 60 and 120 ps at 760 K is shown in figure 7. Their mean values averaged over time (60–120 ps), $\overline{N_T}$ and $\overline{N_O}$, are 69.7 ± 5.5 and 38.3 ± 5.5, respectively. The results show that 35% of Cu ions are distributed among octahedra. Boyce *et al* [12] performed EXAFS experiments on copper halides to investigate their structures and reported that the fraction of Cu ions found in the octahedral sites, c_{oct}, is 30% at 743 K for α-CuI and increases with increasing temperature. The present result that 35% of Cu ions are found in octahedra is in good agreement with their result.

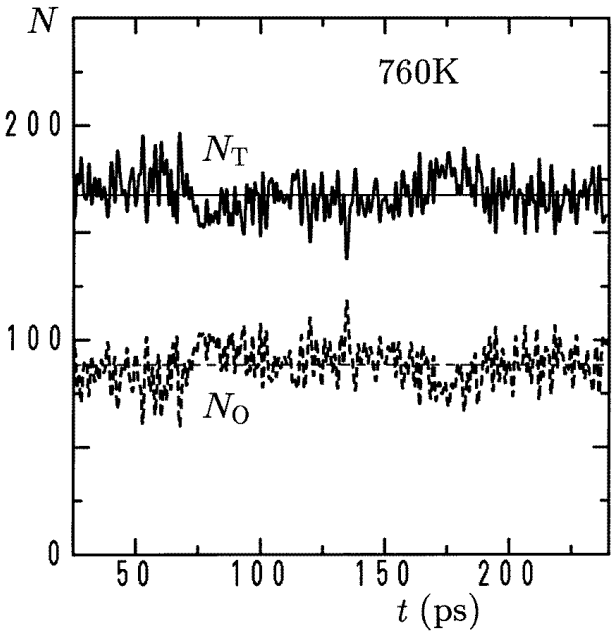

Figure 7. Time dependence of N_T and N_O, which are the numbers of Cu ions inside the tetrahedron and the octahedron, respectively. Horizontal lines represent the respective mean values of N_T and N_O.

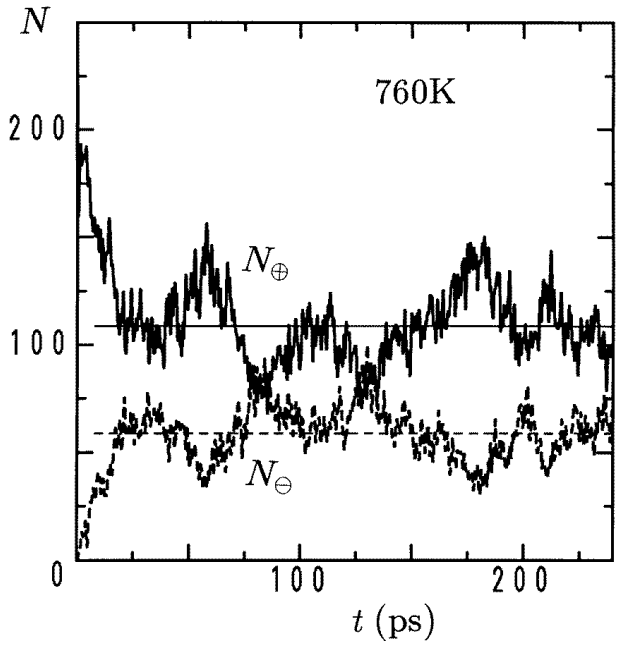

Figure 8. Time dependence of $N_\oplus$ and $N_\ominus$, which represent the numbers of Cu ions inside $\oplus$ and $\ominus$ tetrahedra, respectively, where $N_\oplus + N_\ominus = N_T$.

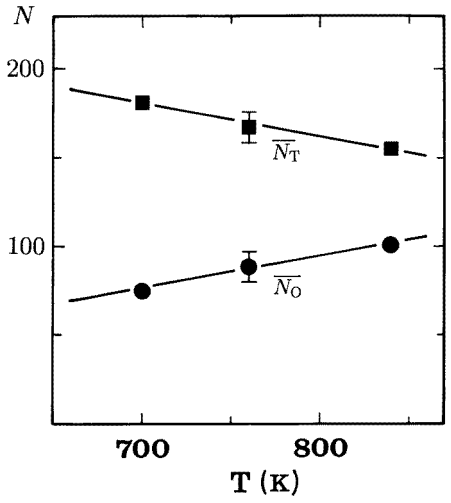

Figure 9. Temperature dependence of $\overline{N_T}$ (full squares) and $\overline{N_O}$ (full circles).

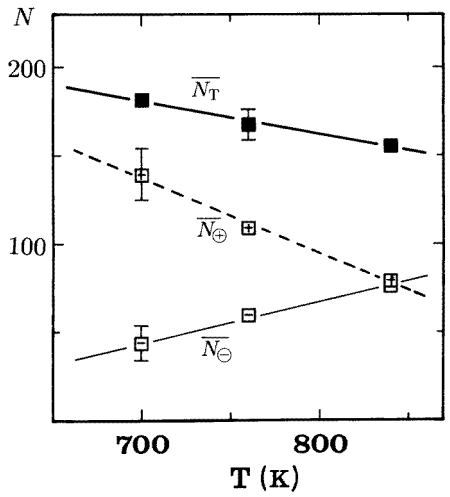

Figure 10. Temperature dependence of $\overline{N_\oplus}$ (⊞), $\overline{N_\ominus}$ (⊟) and $\overline{N_T}$ (■), where $\overline{N_\oplus} + \overline{N_\ominus} = \overline{N_T}$.

65% of Cu ions are distributed among tetrahedra, composed of ⊕ and ⊖ tetrahedra. We examine the numbers of Cu ions found in ⊕ and ⊖ tetrahedra, $N_\oplus$ and $N_\ominus$, in every time step, where $N_\oplus + N_\ominus = N_T$. Figure 8 shows the time variations of $N_\oplus$ and $N_\ominus$ from the initial time to 120 ps at 760 K. During the initial ten time steps, $N_\oplus$ decreases rapidly to about 160 from the initial value 256, and then gradually decreases to about 110 within 20 ps. After 20 ps, $N_\oplus$ and $N_\ominus$ fluctuate around their respective mean values $\overline{N_\oplus}$ and $\overline{N_\ominus}$. The temperature dependences of $\overline{N_T}$, $\overline{N_O}$, $\overline{N_\oplus}$ and $\overline{N_\ominus}$ are shown in figures 9 and 10.

The probability of finding a cation inside a tetrahedron, which changes from 70.3 to 60.5% with increasing temperature, is lower than the occupation probability of a cation at a tetrahedral site (∼86–90%) obtained by Johansson *et al* [6]. This discrepancy stems from the difference in the method of estimation of the probability, that is, in the present work the number of cations inside the tetrahedron is counted while, in their work, each ion is assigned to its closest site. The triangle-sharing tetrahedron and octahedron is situated at one third of the distance from tetrahedral site on the line connecting tetrahedral and octahedral sites. Therefore, an ion which is situated between the triangle and the midpoint of the line is counted as if it belongs to a tetrahedral site, although it is situated inside an octahedron.

4.3. Jump frequency

As described in section 4.1, each Cu ion makes the jump series as follows

$$\cdots \rightarrow \mathrm{T} \rightarrow \mathrm{O} \rightarrow \mathrm{T} \rightarrow \mathrm{O} \rightarrow \cdots \qquad \text{(I)}$$

where T and O stand for tetrahedron and octahedron, respectively.

We evaluate the number of jumps (number of arrows in (I)) in a unit time (jump frequency) Γ for each ion and the distribution of Γ is shown in figure 11. The temperature dependence of the mean value of Γ, $\overline{\Gamma}$, is given in figure 12, where error bars represent the standard deviation of $\overline{\Gamma}$. The diffusion coefficient is related to the jump frequency by the following equation if the diffusion takes place by random walks [13],

$$D = \overline{\Gamma} r^2/6 \qquad (9)$$

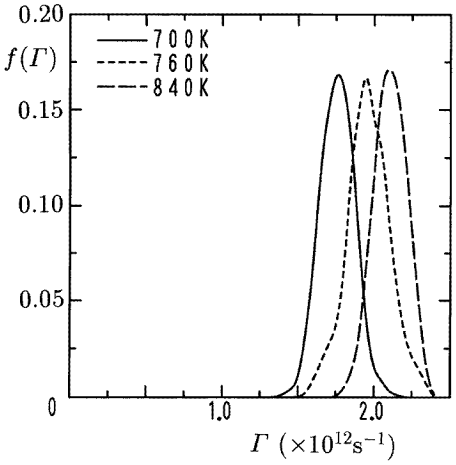

Figure 11. Distribution of the jump frequency of Cu ions at three temperatures. Full, dotted and broken lines are for 700, 760 and 840 K, respectively.

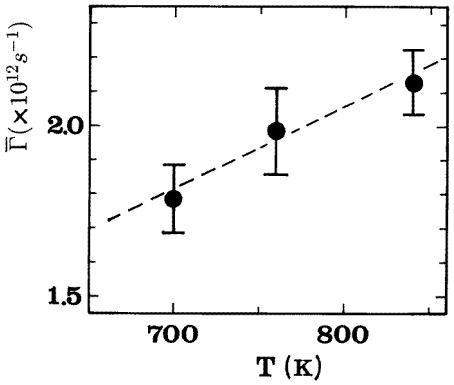

Figure 12. Temperature dependence of the jump frequency of Cu ions. Error bars denote the standard deviations for the distributions shown in figure 11.

where r is the jump distance in each jump. In ordinary solids the temperature dependence of D depends on that of $\overline{\Gamma}$, since r is constant.

If there exists a correlation effect between successive ion jumps, equation (9) is modified as follows,

$$D = \overline{\Gamma} r^2 f/6 \tag{10}$$

where f is called the correlation factor and evaluated by the equation [13, 14]

$$f = (1 + \langle \cos\theta \rangle)/(1 - \langle \cos\theta \rangle) \tag{11}$$

in which θ is the angle formed by two successive jump vectors. $\langle \cos\theta \rangle$ is evaluated from the formula

$$\langle \cos\theta \rangle = \sum_{\alpha} p_\alpha \cos\theta_\alpha \tag{12}$$

if we know p_α, which is the probability with which a jump takes place with an angle θ_α to the preceding jump.

For evaluating $\langle\cos\theta\rangle$, we have to distinguish two types of successive jump in the jump series denoted in (I); one is the jumps T→O→T and the other is O→T→O. From the cation distribution shown in figure 4, we expect that there is a strong correlation between the jump O→T and the preceding jump T → O but no correlation in the jump T → O after the jump O → T, since cations in tetrahedra make vibrational motions around the tetrahedral site and the cation distribution in octahedra is denser when close to the interface between the octahedron and tetrahedron. The situation stated above is approximately realized in α-Ag_2Te [15], whose crystal structure is essentially the same as α-CuI. Therefore, we consider the jumps T→O→T (hereafter abbreviated as a TT jump) in detail.

There are three possibilities for the directions of the TT jumps, namely the [100], [110] and [111] directions. Probabilities that these jumps occur were 89.7, 7.8 and 2.5% at 760 K, respectively. It is known that most of the TT jumps take place in the [100] direction, so we consider only the [100] jump for the evaluation of $\langle\cos\theta\rangle$.

The series of TT jumps is classified into two kinds as shown in the following as an example; one is non-diffusive (backward) and the other diffusive,

$$\cdots \rightarrow \underbrace{\mathrm{T}_A \rightarrow \mathrm{O} \rightarrow \overbrace{\mathrm{T}_A}^{diffusive} \rightarrow \mathrm{O} \rightarrow \mathrm{T}_B}_{backward} \rightarrow \mathrm{O} \rightarrow \underbrace{\mathrm{T}_B}_{backward} \rightarrow \cdots \qquad \text{(II)}$$

where labels $A, B, \ldots$ are used for distinguishing tetrahedra. Probabilities of backward and diffusive jumps, p_{back} and p_{diff} $(=1 - p_{back})$, were examined and their values and temperature dependences were obtained as shown in figure 13. We see that most of the TT jumps are backward jumps.

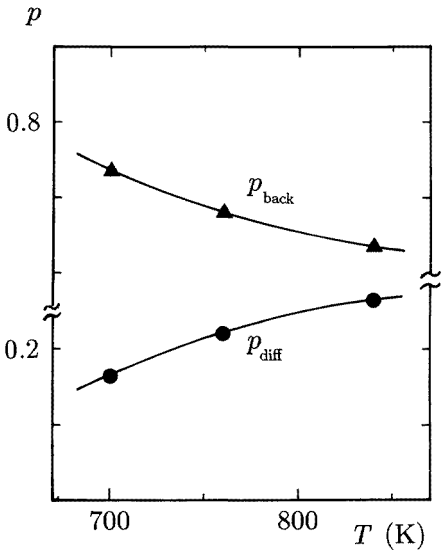

Figure 13. Temperature dependence of probabilities of the backward (non-diffusive) jumps, p_{back}, and diffusive jumps, p_{diff}, where $p_{back} + p_{diff} = 1$. Triangles and circles represent p_{back} and p_{diff}, respectively.

When we consider the [100] jump, the probable angles of θ_α in equation (12) are 0, $\pi/2$ and π, since tetrahedra are arranged in a single cubic form. The case where $\theta_\alpha = \pi$ corresponds to the backward jump and the other cases to diffusive jumps. By assuming that the diffusive jumps with $\theta_\alpha = 0$ and $\pi/2$ occur with equal probability, we evaluated $\langle \cos\ \theta \rangle$ and results are tabulated in table 3.

Table 3. Correlation factors.

	T (K)		
	700	760	840
$\langle \cos\theta \rangle$	−0.802	−0.736	−0.682
f	0.110	0.152	0.189

In ordinary ionic crystals, the diffusion takes place mainly by the vacancy mechanism or by the interstitial mechanism. Then f is definitely determined both by the diffusion mechanism and by the crystal structure and is independent of temperature.

In superionic conductors, however, the crystal structure is so disordered that the diffusion mechanism cannot be simply described by the vacancy or interstitial mechanism. So, f might not be a constant and it is natural to have a temperature dependence, as shown in table 3.

As is shown above, by using the polyhedron analysis method we are able to evaluate the jump frequency and the correlation factor for the diffusion of Cu ions. Using these values, we now examine equation (10). Instead of examining equation (10) directly, we take the logarithm of equation (10):

$$\log D = \log \overline{\Gamma} f + \log(r^2/6).$$

The relation between $\log D$ and $\log \overline{\Gamma} f$ should be expressed by a straight line with an inclination of 45°, if r is a constant. In figure 14, the relation is shown by the full line almost parallel to the broken line, which is drawn with the inclination of 45° against the abscissa.

5. Discussion

Phillips [16] pointed out that the superionic characters of ionic crystals appear when the ionicity of constituent ions, f_i, is not over 0.785 for MX type compounds. When f_i is larger than 0.785, the Coulomb attraction between opposite charged ions is stronger, so that the ion is constrained near opposite charged ions, resulting in no diffusion. However, when f_i is smaller than 0.785, the attractive force between opposite charged ions is weaker and one species of compound becomes movable. In practice, the crystal prefers to have NaCl structure with six coordinations rather than zincblende structure with four coordinations to gain effective electrostatic energy when f_i is over 0.785 [17]. Thus, when the interaction is assumed as in equation (1) the evaluation of the effective valence of constituent ions, z, is important in the MD simulation of superionic conductors.

In earlier work on the MD simulation of CuI, Vashishta and Rahman used $z = 0.60$ and obtained diffusion coefficients larger than experimental ones. In the present calculation, we used $z = 0.70$ and obtained excellent agreement between the calculated and experimental diffusion coefficients. In investigating the simulation, we found the paper of Hennion *et al* [18] in which they report that the phonon dispersion curves for CuI derived from the inelastic

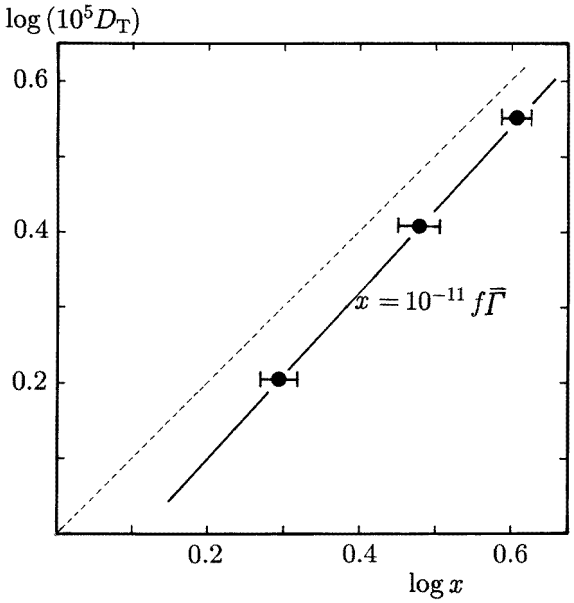

Figure 14. The relation of $\log D$ to $\log f\bar{\Gamma}$.

neutron scattering experiment are well reproduced in terms of a rigid ion model when the effective charge of the Cu ion, q_{Cu}, is taken as $q_{Cu} = 0.69e$. The value $z = 0.70$ was very close to their derived value.

On the problem of the structure of α-CuI, it seems that how Cu ions are distributed is not yet determined definitely because of the high diffusivity and highly disordered distribution of Cu ions, especially on the distribution inside octahedra. Boyce *et al* [12] analysed their EXAFS data in detail by using several structure models such as the anharmonic model, the displaced site model, the excluded volume model and so on, and showed that the best fit to their data is obtained by adjusting a few parameters in the excluded volume model. As described in section 4.2, they concluded that 30% of Cu ions are resident at octahedral sites.

Recently, Keen and Hull [19] performed a neutron diffraction study for CuI powder, in order to refine the crystal structure into its three polymorphisms. They showed that no Cu ions are found to occupy octahedral sites and that the highly disordered distribution appears at a temperature just below the melting temperature. They also pointed out that Cu ions at tetrahedral sites vibrate with a sufficiently large amplitude to penetrate into the octahedra and move to neighbouring tetrahedral sites.

Figure 15 shows the Cu ion density distribution along the [111] direction at 760 K obtained by the present calculation. The figure is figure 4 redrawn along a line from the left-hand end to the right-hand end. Vertical arrows with letters T_+, T_- and O denote the positions of T_+, T_- and octahedral sites, respectively. Dotted arrows denote the positions of the interface triangle between tetrahedra and octahedra. Results obtained by the present calculation are in good agreement with those of Keen and Hull, that is: (i) there are no Cu ions at octahedral sites; (ii) the Cu ion distributions around T_+ and T_- sites penetrate into the octahedra; and (iii) the Cu ion distributions at T_+ and T_- sites are almost equal to each other at 840 K just below the melting temperature, as presumed from figure 8.

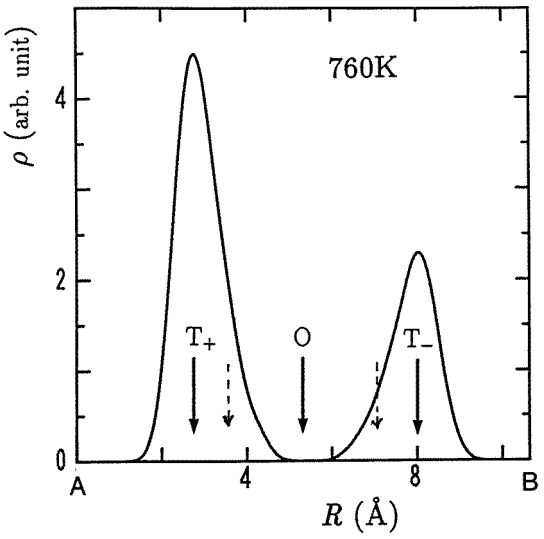

Figure 15. The Cu ion density distribution along the [111] direction at 760 K. Arrows marked by T_+, T_- and O represent positions of the T_+, T_- and octahedral sites, respectively. Dotted arrows denote the positions of the interface between the tetrahedra and octahedra. Letters A and B indicate positions marked in figure 4.

On the other hand, it might be possible to consider that the present results on the Cu ion distribution are in coincidence with those of Boyce *et al* by the following consideration. The Cu ion distribution in an octahedron becomes denser closer to its surface and it is symmetric around an octahedral site. The centre of mass of Cu ions distributed in octahedra must coincide with the octahedral site. Then we might say that Cu ions in octahedra are resident at an octahedral site.

We showed in section 4.3 that equation (10) holds well. However, the relation between $\log D$ and $\log \overline{\Gamma} f$ in figure 14 is not perfectly parallel to the broken line, suggesting that r is dependent slightly on temperature. From equation (10) and calculated values of D, $\overline{\Gamma}$ and f, we can evaluate r and it is obtained as 2.16, 2.21 and 2.30 Å at 700, 760 and 840 K, respectively. The tendency that the penetration distance toward the octahedral site becomes slightly greater with temperature is reasonable. However, these values are fairly small compared to the distance between tetrahedral and octahedral sites, 2.66 Å. This means, as pointed out by Keen and Hull [19], that cations in tetrahedra penetrate toward octahedral sites and go into tetrahedra before reaching octahedral sites.

6. Summary

(1) A constant temperature–constant volume molecular dynamics simulation has been applied to α-CuI with the use of a pairwise interionic potential proposed by Vashishta and Rahman for the same material. The diffusion coefficient of the cation evaluated from the relation between the mean square displacement and time is excellently coincident with the experimental value obtained by a tracer method, by assuming the effective charge of the Cu ion to be $0.70e$ instead of $0.60e$, which is used by Vashishta and Rahman.

(2) The migration behaviour of cations is analysed by the polyhedron analysis method, which describes the position of a mobile ion by a polyhedron including the mobile ion. In α-CuI, about 35% of cations are found in octahedra, which is consistent with the result obtained by EXAFS experiments, where 30% of cations are distributed in octahedral sites. However, in our calculations only a few per cent of cations were found at octahedral sites.

(3) Cations are distributed in tetrahedra and octahedra with probabilities of 70.3 and 29.7% at 700 K, respectively, and the probability of finding a cation in a tetrahedron decreases from 70.3 to 60.5% (840 K) with increasing temperature. Cations in tetrahedra are distributed in $\oplus$ and $\ominus$ tetrahedra with the probability of about 76% ($=p_{\oplus}$) and 24% ($=p_{\ominus}$) at 700 K, respectively. It is realized that $p_{\oplus}$ is almost equal to $p_{\ominus}$ at 840 K, which is close to the melting point of CuI.

(4) Quantities D, $\overline{\Gamma}$ and f derived from the calculating data satisfy consistently the relation $D = \overline{\Gamma} r^2 f/6$, which is realized in ordinary ionic solids.

Acknowledgment

This work is supported by a Grant-in-Aid for Scientific Research on Priority Areas (No 260), 'Dynamics of Fast Ions in Solids and Its Evolution for Solid State Ionics' from the Ministry of Education, Science and Culture of Japan.

References

[1] Vashishta P and Rahman A 1979 *Fast Ion Transport in Solids* ed P Vashishta, J N Mundy and G K Shenoy (New York: North-Holland) p 527
[2] Trullàs J, Giró A, Fontanet R and Silbert M 1994 *Phys. Rev.* B **50** 16 279
[3] Dejus R, Sköld K and Granéli B 1980 *Solid State Ion.* **1** 327
[4] Zheng-Johansson J X M, Sköld K and Jørgensen J E 1992 *Solid State Ion.* **50** 247
[5] Zheng-Johansson J X M, Ebbsjö I and McGreevy R L 1995 *Solid State Ion.* **82** 115
[6] Zheng-Johansson J X M and McGreevy R L 1996 *Solid State Ion.* **83** 35
[7] Hoover W G 1985 *Phys. Rev.* A **31** 1695
[8] Miyake S, Hoshino S and Takenaka T 1952 *J. Phys. Soc. Japan* **7** 19
[9] Hokazono M, Ueda A and Hiwatari Y 1984 *Solid State Ion.* **13** 151
[10] Tachibana F, Kobayashi M and Okazaki H 1988 *Solid State Ion.* **28–30** 41
Tachibana F, Kobayashi M and Okazaki H 1989 *Solid State Ion.* **35** 349
[11] Shimojo F and Okazaki H 1992 *J. Phys. Soc. Japan* **61** 4106
[12] Boyce J B, Hayes T M and Mikkelsen J C Jr 1981 *Phys. Rev.* B **23** 2876
[13] Shewmon P G 1963 *Diffusion in Solids* (New York: McGraw-Hill)
[14] Leclaire A D 1970 *Physical Chemistry* vol 10 (London: Academic)
[15] Tachibana F, Sakai Y and Okazaki H 1992 *J. Phys.: Condens. Matter* **4** 8989
[16] Phillips J C 1976 *J. Electrochem. Soc.* **124** 934
[17] Phillips J C 1973 *Bonds and Bands in Semiconductors* (New York: Academic) ch 2
[18] Hennion B, Moussa F, Prevot B, Carabatos C and Schawb C 1972 *Phys. Rev. Lett.* **28** 964
[19] Keen D A and Hull S 1995 *J. Phys.: Condens. Matter* **7** 5793